analytical chemistry

Article

pubs.acs.org/ac

Gas-Phase FRET Efficiency Measurements To Probe the Conformation of Mass-Selected Proteins

Martin F. Czar,[§] Franziska Zosel,[†] Iwo König,[†] Daniel Nettels,[†] Bengt Wunderlich,[†] Benjamin Schuler,[†] Arash Zarrine-Afsar,*[,†,‡] and Rebecca A. Jockusch*[,§]

[§]Department of Chemistry, University of Toronto, Toronto, Ontario M5S 3H6, Canada

[†]Biochemisches Institut, Universität Zürich, Zürich, CH-8057, Switzerland

Supporting Information

ABSTRACT: Electrospray ionization and mass spectrometry have revolutionized the chemical analysis of biological molecules, including proteins. However, the correspondence between a protein's native structure and its structure in the mass spectrometer (where it is gaseous) remains unclear. Here, we show that fluorescence (Förster) resonance energy transfer (FRET) measurements combined with mass spectrometry provides intramolecular distance constraints in gaseous, ionized proteins. Using an experimental setup which combines trapping mass spectrometry and laser-induced fluorescence spectroscopy, the structure of a fluorescently labeled mutant variant of the protein GB1 was probed as a function of charge state. Steady-state fluorescence emission spectra and time-resolved donor fluorescence measurements of mass-selected GB1 show a marked decrease in the FRET efficiency with increasing number of charges on the gaseous protein, which suggests a Coulombically driven unfolding and expansion of its structure. This lies in stark contrast to the pH stability of GB1 in solution. Comparison with solution-phase single-molecule FRET measurements show lower FRET efficiency for all charge states of the gaseous protein examined, indicating that the ensemble of conformations present in the gas phase is, on average, more expanded than the native form. These results represent the first FRET measurements on a mass-selected protein and illustrate the utility of FRET for obtaining a new kind of structural information for large, desolvated biomolecules.

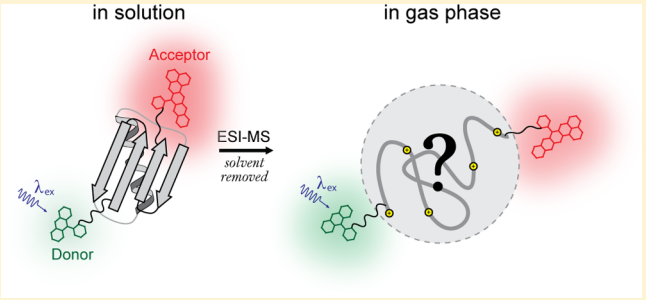

The combination of soft ionization methods such as electrospray ionization (ESI)[1,2] and trapping mass spectrometry (MS) has enabled detailed studies on the reactivity and structure of proteins in the gas phase. However, better understanding the transferability of physical and chemical properties measured *in vacuo* to their native (*in vivo*) or near-native environments remains an intense area of research.[3,4] This research is motivated largely by two factors. First, determining how, and under what conditions, a desolvated protein's structure is different from what is found in nature may reveal the structural importance of those interactions which are removed upon transfer to the gas phase. Further, inferences drawn based upon MS data about solution-phase properties demand a clear understanding of the relationship between the solution- and gas-phase behavior of proteins. The available tools to study gas-phase structure in proteins, including those relying on ion mobility,[5] deuterium exchange,[6] and ion dissociation,[7,8] have been used to glean significant insight: electrosprayed proteins carrying a relatively low number of charges often retain facets of their solution structure, whereas those carrying more charge lose these characteristics. Furthermore, larger proteins and protein assemblies appear to be more likely to retain structure upon electrospray ionization than their smaller counterparts, perhaps due to enhanced kinetic trapping of the larger systems. Despite these advances, the richness in structural detail that is routinely attainable for proteins in solution is lacking for gaseous proteins due to the limitations of available tools for gas-phase structural characterization. Here, we show that spectral (dispersed) and time-resolved fluorescence (or Förster) resonance energy transfer (FRET) measurements can be used to obtain intramolecular distance constraints in gaseous protein ions.

FRET is the nonradiative transfer of electronic energy from an excited donor dye to an acceptor dye in its ground state and occurs through dipole−dipole interactions.[9,10] This process results in a quenching of donor fluorescence, sensitized emission from the acceptor, and a transfer rate which depends strongly (inverse sixth-power) on the distance between the dyes. Thus, the efficiency of energy transfer, which encodes structural information, can be assessed both by steady-state spectral fluorescence measurements and by measurement of time-resolved fluorescence. The latter is generally regarded as more robust for the determination of FRET efficiencies. The effective working distance of FRET is in the range of 2−10 nm,

Received: April 27, 2015
Accepted: June 25, 2015
Published: June 25, 2015

DOI: 10.1021/acs.analchem.5b01591
Anal. Chem. 2015, 87, 7559−7565

which spans well the dimensions of many biological systems; FRET has thus become a popular way to study biological processes in solution, including protein folding[11−13] and protein−protein interaction.[14] The exquisite sensitivity of FRET makes it well-suited for studying protein dynamics in solution on the submicrosecond to millisecond time scales at the single-molecule level;[13] this sensitivity also makes it an attractive choice for gas-phase analysis, where low ion density and low light collection efficiency forestall the use of less sensitive optical methods.

In the gas phase, FRET has so far only been applied to study small, model systems. Seminal work reported in 2003 by the group of J. H. Parks employed FRET to probe the temperature-dependent unzipping of complementary 14-mer oligonucleotides in a quadrupole ion trap mass spectrometer.[15] Subsequent work from the Zenobi lab utilized a FRET scheme to probe short synthetic polymers in a Penning trap.[16] Both of these early works relied on measurement of total donor fluorescence, from which FRET efficiencies (and thus interdye distances) could not be obtained. The main challenge to the measurement of gas-phase FRET efficiencies is the collection of sufficient fluorescence signal that the light may be spectrally dispersed and/or that time-resolved measurements may be performed in a reasonably efficient manner. This challenge generally grows with the size of the system examined because space charge limits the total density of charges which may be trapped,[17] and larger systems (at least those transferred to the gas phase via ESI) generally carry more charges. Recently, an elegant "action-FRET" strategy was proposed by the Dugourd group as a means to circumvent the need for optical detection.[18] While action FRET shows promise and is more easily implemented than traditional FRET, optical detection has the distinct advantage of providing a way to resolve multiple conformational populations which display different FRET efficiencies, i.e., via time-resolved fluorescence measurements. This was shown recently by our group in a study on dye-labeled model peptides containing 8, 14, and 20 prolines,[19] which also reported the first values of gas-phase FRET efficiencies.

Here, we report the first FRET measurements of a gaseous ionized protein, namely, a 59-residue variant of the immunoglobin G-binding domain of protein G (GB1) (sequence shown in the Supporting Information). It has a common (ubiquitin-like) structural motif comprised of a four-stranded β-sheet, which is spanned by a single α-helix, thus forming a densely packed hydrophobic core (Scheme 1).[20] The

Scheme 1. X-ray Crystal Structure of GB1 (from 1PGA)[20] with Modifications for Fluorescent Labeling Indicated

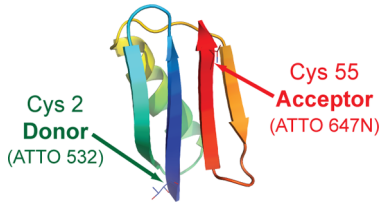

structural and dynamic properties of GB1 have been studied in detail in the condensed phase, notably by X-ray crystallography,[20] nuclear magnetic resonance spectroscopy,[21−24] stopped-flow kinetics experiments,[25−27] differential scanning calorimetry,[28] and computational methods.[29] GB1 has high thermal stability, with a melting temperature of 87.5 °C at pH 5.4,[28] and it retains its native fold over a broad pH range (1.5−11).[25] The solution-phase stability of GB1 has been attributed to its high secondary structure content (∼95%) and the amphiphilic helix which is involved in the formation of its hydrophobic core.[21,24,28] These features led us to ask whether the fold of GB1 remains intact in the gas phase, where removal of solvent may be expected to shift the balance of the enthalpic and entropic contributions which maintain its native fold.

The gas-phase FRET experiments described below use a combination of electrospray ionization, trapping mass spectrometry, and fluorescence spectroscopy to probe the gas-phase structure of a fluorescently labeled mutant variant of the protein GB1. The FRET efficiency of the gaseous protein is investigated as a function of charge state using both dispersed (spectral) fluorescence measurements and time-resolved fluorescence from the donor dye. Gas-phase FRET efficiencies, and derived distance constraints, are compared with results from solution-phase single-molecule FRET experiments.

EXPERIMENTAL SECTION

To enable gas-phase FRET investigations, a GB1 variant was employed which has two residues substituted with cysteine near its termini, at Asn 2 and Thr 55. These residues are located within beta strands and are surface exposed, so these substitutions should be relatively benign.[30] The substitutions enabled site-selective labeling with two thiol-reactive dyes: ATTO 532 (donor, D) and ATTO 647N (acceptor, A) (Scheme 1, protocol in the Supporting Information, Figure S-1). The conjugate GB1-D contains only the donor dye, whereas GB1-DA has both donor and acceptor labels.

Fluorescence emission spectra and lifetime measurements of gaseous GB1 conjugates employed a mass spectrometry setup with modifications to enable spectroscopic investigations of mass-selected gaseous ions.[31−33] Central to the setup is a quadrupole ion trap mass spectrometer (QIT, *Esquire 3000+*, Bruker Daltonics, Bremen, Germany) which has holes drilled in the ring electrode for optical access. The use of a QIT enables confinement of a relatively large number of mass-selected ions (up to ∼100 000) for up to 20 s in a much smaller (∼0.1 mm^3) volume[34] than other types of trapping mass spectrometers, which facilitates the collection of fluorescence. The trade-off for the relatively high fluorescence signal achievable with the high ion densities in our setup is a reduction of mass resolving power of the QIT, which is already substantially lower than that of Orbitraps and Penning traps. Ions trapped in the QIT are irradiated with UV/visible light (tunable from 350−530 nm) generated by frequency-doubling the output of a pulsed (∼130 fs pulse duration, 80 MHz repetition rate) titanium:sapphire laser (*Tsunami*, Spectra-Physics, Newport Co., Mountainview, USA). This choice of laser system was guided by the need for both wavelength tunability and a pulsed source with a high repetition rate. The latter is critical for efficient measurement of fluorescence lifetimes using time-correlated single-photon counting (TCSP) techniques, which we employ due to their compatibility with low levels of light.[33]

Nanoelectrospray ionization (nano-ESI)[2] was used to deliver GB1 conjugates with multiple sodium adducts (of type $[\text{GB1-DA} + m\text{Na} - (m \mp n)\text{H}]^{n\pm}$) to the mass spectrometer (experimental details in the Supporting Information). These were trapped, and mass selection was used to isolate complexes with a known number of charges. These complexes were then irradiated for 0.5−10 s using 485 nm light (∼10 mW, fwhm = 3.5 nm). Fluorescence emission spectra were measured during

DOI: 10.1021/acs.analchem.5b01591
Anal. Chem. 2015, 87, 7559−7565

the irradiation period by focusing the collected fluorescence light onto the entrance slit of a spectrograph interfaced with an electron-multiplying charge-coupled device (*Shamrock 303i* and *Newton* EM-CCD, Andor Technologies, Belfast, Ireland). Donor fluorescence lifetimes were measured using TCSPC techniques by focusing filtered fluorescence light onto a single-photon avalanche diode (*PDM-100*, Micro Photon Devices, Bolzano, Italy) detector, whose output is sent to a TCSPC card (*TimeHarp 200*, Picoquant, Berlin, Germany). After each irradiation period, a mass spectrum was recorded to ensure that significant photodissociation or electron photodetachment did not occur. Gas-phase fluorescence data shown were acquired from interrogating hundreds of populations of trapped ions and subtracting background light levels measured without ions present. To complement gas-phase experiments, solution-phase single-molecule FRET experiments were carried out on GB1-DA using an experimental setup described previously[35] (see the Supporting Information for details).

RESULTS AND DISCUSSION

Figure 1 shows typical nano-ESI mass spectra, measured in positive ion mode, of protein GB1 containing donor and acceptor labels (GB1-DA) before (top) and after (bottom) isolation of a single charge state. The appearance of the nano-ESI mass spectrum, which features a narrow distribution of charge states centered around the 5+ state, suggests the presence of a folded protein in solution (i.e., at the beginning of the ESI process).[36] The noticeable envelope of peaks within each charge state (inset) corresponds to multiple (0−13) sodium adducts; this was verified by high resolution Fourier-transform ion cyclotron resonance mass spectrometry. The extent of sodium adduction reflects the presence of sodium phosphate in the electrosprayed solution. Solutions without sodium phosphate produced a similar charge-state distribution (Figure S-2, Supporting Information); however, the ESI signal from solutions lacking sodium was not stable for long enough to perform gas-phase fluorescence measurements.

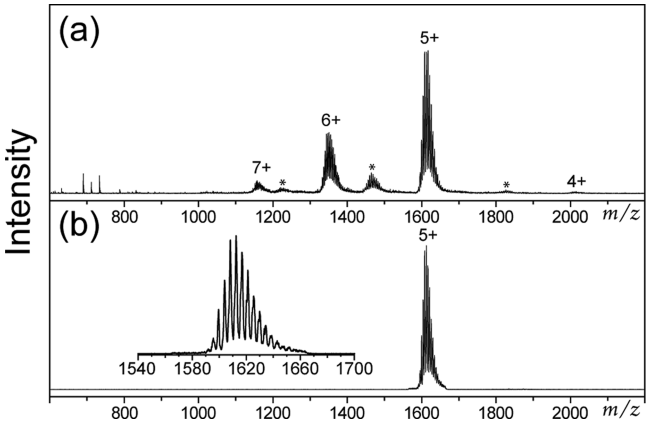

Figure 1. Nanoelectrospray ionization mass spectra of 1 μM GB1-DA in 30 mM ammonium acetate, 0.5 mM sodium phosphate, 80:20 water/methanol. (a) Mass spectrum without ion isolation; the charge states of GB1-DA observed are indicated. Peaks marked with an asterisk (*) correspond to the donor-only conjugate GB1-D present in the sample. (b) Mass spectrum measured after isolation of the 5+ charge state of GB1-DA. Inset is an expansion showing multiple sodium adducts.

Figure 2a−e shows gas-phase fluorescence emission spectra measured for a range of charge states (4+−8+) of GB1-DA generated by positive nano-ESI. There are two bands in all spectra, with maxima at 539 and 640 nm, corresponding to donor and acceptor emission, respectively. Measured spectra of the control donor-only labeled conjugate GB1-D (Figure S-3a, Supporting Information) show a single band at 539 nm, whereas spectra of GB1-A show negligible intensity under the same conditions, indicating that the excitation wavelength used (485 nm) selectively excites the donor. Emission spectra for the 4+ and 5+ states are similar (Figure 2a,b) and indicate a high FRET efficiency, with both showing predominantly sensitized emission from the acceptor, and low intensity from the donor. In contrast, the 6+, 7+, and 8+ states (Figure 2c−e) show a consistent decrease in FRET efficiency with increasing charge, as evidenced by a progressive recovery of donor fluorescence, and a concomitant decrease in acceptor emission intensity. In the 8+ state, very little energy transfer is observed. These results suggest that the higher charge state (6+, 7+, 8+) conformational ensembles represent GB1-DA structures in which the termini of the protein are progressively farther apart with increasing charge, whereas the two lowest charge states examined (4+, 5+) represent structures which are on average more compact. The charge-state dependence of FRET efficiency is similar to that observed previously by our group in small polyproline peptides of intermediate length (14 repeats)[19] and is in accordance with the view of an expansion of the protein's conformation driven by electrostatic repulsion. This effect is magnified in the gas phase due to the absence of charge screening, which is provided by solvent in the condensed phase. Although there are no reports of gas-phase structural studies of GB1 to allow comparison of these data, a clear comparison can be drawn with ion mobility measurements on the protein ubiquitin,[37] which is a protein of similar size and structural topology to GB1. The collision cross section of ubiquitin increases by ∼50% as its charge state increases from 4+ to 8+, shifting from a cross section that is marginally larger than that of the crystal structure to an elongated conformation.

FRET provides an additional nonradiative decay channel for the donor to return to the ground state and manifests as a shortening of the donor fluorescence lifetime. Fluorescence time-decays measured for the donor channel (isolated using a 506−594 nm band-pass filter) for the 5+, 6+, and 7+ charge states of gaseous GB1-DA are shown in Figure 2f−h, with fits shown in green. Donor lifetimes are clearly shorter in the presence of the acceptor than in its absence (i.e., in GB1-D), where the lifetime is ∼7.9 ns (overlaid gray traces). Furthermore, the measured decay depends on charge state for GB1-DA, while it is insensitive to the charge state for GB1-D (Figure S-3b−e, Supporting Information). Lifetimes extracted from fits to the time-resolved data are listed in Table 1. The 5+ state (Figure 2f) exhibits a clear multi-exponential decay, with a fast major decay component (62% from fitted amplitude) with a lifetime of 1.05 ± 0.11 ns, and a slower minor component (30% from fitted amplitude) with a fitted lifetime of 4.3 ± 1.5 ns. The remaining 8% fitted amplitude corresponds to a component included in the fit with a lifetime fixed at 7.9 ns. This was done in order to account for the possibility of a population that is FRET-inactive due, e.g., to residual inactivation of the acceptor by intramolecular electron transfer,[38] which if present and unaccounted for, would result in erroneously long fitted lifetimes. The data suggest that at least two conformational ensembles are resolved in the isolated 5+

DOI: 10.1021/acs.analchem.5b01591
Anal. Chem. 2015, 87, 7559−7565

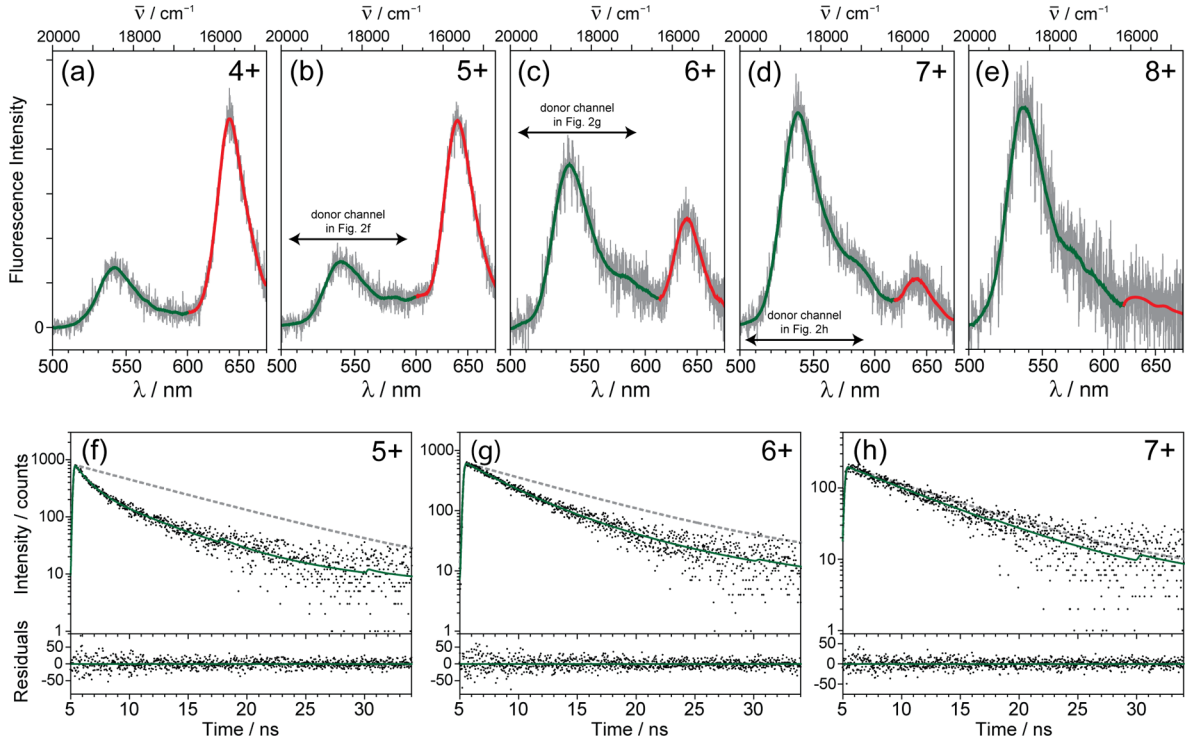

Figure 2. Charge-state resolved emission spectra (a–e) and donor band time-resolved fluorescence (f–h) of fluorescently labeled gaseous GB1-DA conjugates produced by nanoelectrospray ionization and excited with 485 nm light. Smoothed lines in spectra highlight the donor (green) and acceptor (red) emission bands. The wavelength range transmitted by the band-pass filter used in donor lifetime measurements is indicated. Fits to the time-resolved data (f–h, solid curves) are multiexponential functions convolved with a Gaussian instrument response function of adjustable width (~0.2 ns). The extracted fit parameters are shown in Table 1. A small amount of secondary excitation at 12.5 ns intervals, due to incomplete pulse picking, is visible as small bumps in the time-resolved data and has been accounted for in the fit. More slowly decaying traces (dashed gray lines) show the longer lifetime of the donor-only construct, GB1-D (see the Supporting Information).

Table 1. Computed Gas-Phase FRET Efficiencies (E) and Inter-Dye Distance Estimates (r_{DA}) for Different Charge States of GB1-DA

	fluorescence spectra		time-resolved donor fluorescence			
charge state	E^a	$r_{DA}{}^b$ (Å)	relative amplitude	lifetime (ns)	E^a	$r_{DA}{}^b$ (Å)
4+	0.77 ± 0.05	54 ± 4	–	–	–	–
5+	0.76 ± 0.05	55 ± 4	A_1 = 0.62 ± 0.07	τ_1 = 1.05 ± 0.11	E_1 = 0.87 ± 0.02	r_{DA1} = 45 ± 2
			A_2 = 0.30 ± 0.07	τ_2 = 4.3 ± 1.5	E_2 = 0.44 ± 0.21	r_{DA2} = 90 ± 30
			$A_0{}^d$ = 0.08 ± 0.11		$E_{avg}{}^c$ = 0.72 ± 0.20	
6+	0.38 ± 0.06	94 ± 8	A_1 = 0.71 ± 0.06	τ_1 = 3.35 ± 0.21	E_1 = 0.57 ± 0.04	r_{DA1} = 72 ± 4
			$A_0{}^d$ = 0.29 ± 0.05		$E_{avg}{}^c$ = 0.32 ± 0.14	
7+	0.14 ± 0.03	150 ± 15	–	τ_1 = 6.59 ± 0.22	0.16 ± 0.07	150 ± 30
8+	0.06 ± 0.02	>170	–	–	–	–
4–	0.89 ± 0.03	43 ± 3	–	–	–	–
5–	0.83 ± 0.05	49 ± 5	–	–	–	–

[a]Procedures for calculations are outlined in the Supporting Information. [b]Calculated using measured FRET efficiencies (E), a Gaussian chain model,[41] and $R_{0,gas}$ = 72 ± 1 Å (see the Supporting Information). [c]Amplitude-weighted average. [d]Relative amplitude of FRET-inactive component, with lifetime fixed at 7.9 ns. This component was not resolvable for the 7+ state, due to its long fluorescence lifetime and relatively low signal-to-noise.

state of GB1-DA: the majority of ions have fast energy transfer due to their relatively compact structures, but a significant fraction have more expanded conformations. Fits to the 6+ data resolve only a single population displaying FRET, with a lifetime of 3.35 ± 0.21 ns. This falls within the uncertainty of the slower minor component from the 5+ data. The 7+ data are fit well by a single exponential decay with a significantly longer lifetime of 6.6 ns. Overall, fits to the time-resolved data are consistent with the fluorescence emission spectra (Figure 2a–e), again indicating that the FRET efficiency decreases as the number of charges present on the protein increases. However, analysis of time-resolved data can reveal the presence of multiple conformations, as it does here for the 5+ charge state, information not attainable from steady-state spectra alone. We note that the analysis presented here used a discrete number of (up to three) lifetime components. Time-resolved fluorescence from an ensemble of conformations is better modeled using a continuous interdye distance distribution function; however, given the relatively low signal-to-noise for these gas-phase fluorescence measurements, such treatment was not feasible.

DOI: 10.1021/acs.analchem.5b01591
Anal. Chem. 2015, 87, 7559–7565

We have also examined the fluorescence properties of two charge states of GB1-DA generated by negative nano-ESI (Figure 3). Both anionic charge states show sensitized emission

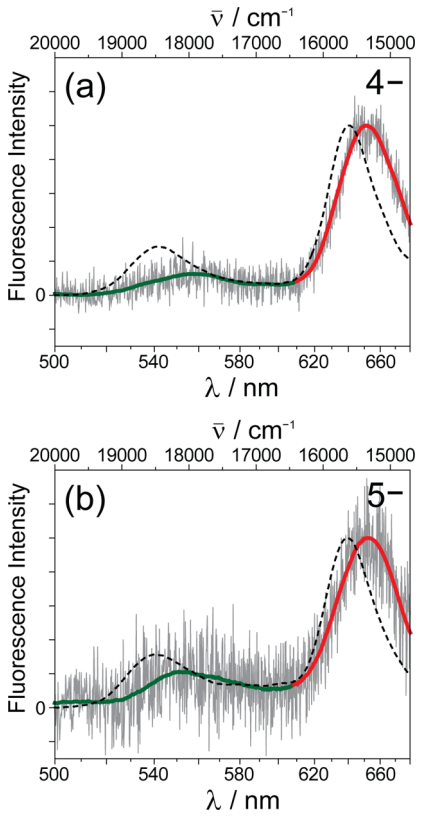

Figure 3. Fluorescence emission spectra (gray traces) for 4− (a) and 5− (b) charge states of GB1-DA, excited using 485 nm light. Smoothed lines highlight donor (green) and acceptor (red) emission bands. Smoothed emission spectra of the 4+ (a) and 5+ (b) states (dashed lines) are overlaid for comparison.

from the acceptor, with a smaller band corresponding to fluorescence from the donor. The emission maxima of the donor and acceptor dyes are shifted to somewhat lower energy, by 500 and 200 cm^{-1}, respectively, than their cationic counterparts. The FRET efficiencies in the 4− and 5− states are slightly higher than those of the 4+ and 5+ states, suggesting anionic GB1-DA conformers which are perhaps marginally more compact than the cations.

The signal-to-noise in the emission spectra measured for the anionic GB1-DA species (Figure 3), and also for the higher charge states of the cations (Figure 2c−e), is noticeably worse than in the spectra measured for lower charge states of cationic GB1-DA (*cf.* Figure 2a,b). In the case of the anions, this is a result of facile electron photodetachment (*e*PD)[39] from negatively charged GB1-DA, which is discernible in the measured mass spectrum. This is not unexpected, as the photon energy (2.55 eV) at the irradiation wavelength used is sufficient to detach electrons from other multiply charged anionic proteins with similar charge density, in both highly folded and elongated conformations.[40] Unfortunately, the facile *e*PD reduces the maximum allowable irradiation time significantly in these experiments (~0.5 s, *cf.* 10 s irradiation for the 4+ and 5+ charge states), which hinders the duty cycle of fluorescence measurements. FRET measurements of the more highly charged cations (6+, 7+, 8+) similarly suffer from duty cycle limitations, although in this case too much irradiation results in undesired photofragmentation rather than electron detachment. The significantly lower relative abundances for the higher charge states (as expected for an electrosprayed protein under "native" solution conditions; see Figure 1) also decreased the signal-to-noise of the 7+, and 8+ charge states.

The structural information we seek (i.e., interdye distances) depends on the FRET efficiency (E), which can be calculated from emission spectra or more reliably from the donor fluorescence lifetimes (Table 1; see the Supporting Information for calculations). In cationic GB1-DA, the FRET efficiency computed from spectra is highest for the 4+ and 5+ states (~0.8), lies at an intermediate value for the 6+ state (~0.4), and then declines to below 0.2 for the 7+ and 8+ states. In the 4− and 5− states, the efficiencies lie near 0.9 and 0.8, respectively. Interdye distances (r_{DA}) for gaseous GB1 were calculated according to Förster theory[9,10] and using a Gaussian chain model.[41] Central to calculating r_{DA} is the Förster radius (R_0), which is the distance at which $E = 0.5$. R_0 for a given dye pair depends upon the spectroscopic properties of the dyes and on their chemical environment. In aqueous solution, R_0 for this dye pair is 59 Å (Atto Tec GmbH); however, its gas-phase value is unknown. Making reasonable assumptions, we estimate $R_{0,gas}$ for this dye pair to be 72 Å (see the Supporting Information for details). This is significantly larger than the solution-phase value due mainly to the lower index of refraction in vacuum ($n_{vacuum} = 1$, while $n_{aq} \approx 1.33$ at 530 nm). We note that the largest uncertainty in our estimate of $R_{0,gas}$ is the orientation factor κ^2, which describes the relative orientation of the donor and acceptor transition dipoles. In solution, polarization anisotropy decay measurements can be used to assess the rotational mobility of a FRET pair,[10] but this is not accessible in our gas-phase experiments. Instead, we have assumed here the dynamically averaged value of $\kappa^2 = 2/3$, as is often done in solution-phase studies. However, the dyes may not be freely rotating in this gas-phase system, especially given that they are charged (see the Supporting Information for further discussion).

Table 1 shows estimates of interdye distances (r_{DA}) for the various charge states of gaseous GB1-DA, computed using measured FRET efficiencies and the estimated $R_{0,gas}$ value of 72 Å. Estimates range from 40−60 Å for the lowest charge states examined (4+, 5+, 4−, 5−) and are >70 Å for the 6+, 7+, and 8+ states. All of these distances are longer than the interdye distance for the folded protein in the condensed phase as determined by aqueous-phase single-molecule FRET experiments. In aqueous solution at pH 7 and 2.5, energy transfer is virtually complete (Figure S-4, Supporting Information). FRET efficiency histograms suggest values of $r_{DA} < 30$ Å for the folded protein in solution, which agrees well with the inter-residue distance of the dye labeling sites based on the X-ray crystal structure of GB1 (21 Å),[20] plus a correction for the lengths of the dye−protein linkers used. The >70 Å interdye distances in the higher charge states examined (6+, 7+, 8+) and in the expanded population of the 5+ state suggest gaseous GB1 conformations which are significantly expanded relative to its native fold. The sites of dye attachment are 53 residues apart; for comparison, an α-helix of this length would be 79.5 Å.

Just how compact are the populations identified here as relatively compact? Overall, the estimates of r_{DA} may indicate that, even in the most compact gaseous GB1 conformers probed, the sites of dye attachment (which lie on β-strands 1

DOI: 10.1021/acs.analchem.5b01591
Anal. Chem. 2015, 87, 7559−7565

and 4) are not in as close proximity as they are in the folded structure (Scheme 1). The higher efficiency of energy transfer observed for the anionic charge states compared to the most compact cationic charge states supports the idea that the 4+ and more compact 5+ population are more expanded than the native structure in solution. However, given the remaining uncertainties in the orientational freedom of the dyes, the signal-to-noise of the time-resolved data, and inherent challenges of multiexponential fitting, as well as the possibility of residual inactivation of the acceptor by electron transfer,[38] it may be that the most compact gaseous GB1 conformers are indeed close in compactness to the native solution structure. Furthermore, we cannot rule out the possibility that the analysis used for the lifetime data might miss a minor very high FRET component due to its very fast decay. Experiments designed to address this possibility are currently underway in our laboratory. Nonetheless, with increasing number of charges per molecule, a clear transition to unfolded and increasingly expanded conformations is evident, to an extent that prevents energy transfer almost completely.

The gas-phase behavior of GB1-DA lies in contrast to the stability of its fold in solution. The pH stability of wild type GB1[25] translates to stability over charge states in solution ranging approximately from 13− to 7+, assuming standard amino acid pK_a values. Single-molecule FRET data indicate that the fluorescently labeled mutant variant used here is, like the wild type, folded at neutral pH and under acidic conditions (Figure S-4b, Supporting Information). The narrow charge-state distribution and low overall degree of charging observed in the ESI mass spectrum (Figure 1) are consistent with the presence of a folded protein at the start of the ESI process, in agreement with single-molecule data measured in ESI buffer (Figure S-4c, Supporting Information). The gas-phase FRET data shown here suggest that the desolvation and charging processes lead to a disruption of the tertiary structure of GB1-DA on the time scale of these experiments. In some ways, this is not surprising as GB1 lacks several features which favor retention of native-like structure in the gas phase, including disulfide bonds that stabilize tertiary structure and the kinetic stability (arising from the internal energy bath) associated with larger proteins and complexes. Moreover, the energy barrier for unfolding is likely to be lower in the gas phase than in solution due to the enhanced Coulomb repulsion upon desolvation of this small protein.[42] This, combined with the seconds-long irradiation period used in these gas-phase FRET experiments, which are quite long by mass spectrometry standards, could give many small proteins sufficient time to rearrange.

CONCLUSIONS

This work adds a technique complementary to the methods currently available to probe the conformation of mass-selected biomolecules. FRET efficiency measurements provide a probe of interdye distances, which here show the expansion with increasing charge state of the conformation of the small gaseous protein GB1-DA, pointing to a Coulombically-driven structural change in the absence of solvent. Moreover, time-resolved measurements indicate the presence of both expanded and relatively compact conformers for the 5+ charge state.

While the necessity of appropriate labels for FRET experiments is a drawback of this technique, FRET-based strategies are remarkably powerful. Their use in the gas phase will make it possible to access new information about biomolecules. FRET is intrinsically very sensitive to changes in interdye distance near the Förster radius (R_0) for the FRET pair used. Using careful selection of labeling sites, FRET methods can be adapted to target substructural changes via the incorporation of paired labels at different sites, in order to give insight into the cooperativity of structural transitions.[43,44] Furthermore, use of a three-color FRET strategy makes possible the measurement of two distances in concert.[45] We anticipate that distance constraint information obtained using gas-phase FRET will assist computational efforts aimed at larger systems. Ultimately, since relatively little is known about protein folding in the complete (or partial) absence of solvent, we envision using gas-phase FRET of mass-selected proteins and clusters to study several aspects of protein folding, including how destabilizing point mutations translate to the gas phase and how the addition of a well-defined number of water molecules affects protein folding and stability.

ASSOCIATED CONTENT

Supporting Information

GB1 synthesis; mass spectra; donor-only control experiments; calculations; single-molecule FRET experiments. The Supporting Information is available free of charge on the ACS Publications website at DOI: 10.1021/acs.analchem.5b01591.

AUTHOR INFORMATION

Corresponding Authors

*Tel: +1-416-581-8473. E-mail: arash.zarrine.afsar@utoronto.ca.

*Tel: +1-416-946-7198. E-mail: rjockusc@chem.utoronto.ca.

Present Address

‡(A.F.-A.) Techna Institute for the Advancement of Technology for Health, University of Toronto, Toronto, Ontario M5G 1P5, Canada

Notes

The authors declare no competing financial interest.

ACKNOWLEDGMENTS

M.F.C. and R.A.J. are grateful for funding from the Natural Sciences and Engineering Research Council of Canada, the Canada Research Chairs Program, the Canada Foundation for Innovation, and the Province of Ontario. This work was also supported by the Human Frontier Science Program (to A.Z.-A.) and the Swiss National Science Foundation (to B.S.).

REFERENCES

(1) Fenn, J. B.; Mann, M.; Meng, C. K.; Wong, S. F.; Whitehouse, C. M. *Mass Spectrom. Rev.* **1990**, *9* (1), 37−70.
(2) Wilm, M.; Mann, M. *Anal. Chem.* **1996**, *68* (1), 1−8.
(3) Ruotolo, B.; Robinson, C. *Curr. Opin. Chem. Biol.* **2006**, *10*, 402−408.
(4) Breuker, K.; McLafferty, F. W. *Proc. Natl. Acad. Sci. U. S. A.* **2008**, *105* (47), 18145−18152.
(5) Bohrer, B. C.; Merenbloom, S. I.; Koeniger, S. L.; Hilderbrand, A. E.; Clemmer, D. E. *Annu. Rev. Anal. Chem.* **2008**, *1* (1), 293−327.
(6) Wood, T.; Chorush, R.; Wampler, F.; Little, D.; O'Connor, P.; McLafferty, F. *Proc. Natl. Acad. Sci. U. S. A.* **1995**, *92* (7), 2451−2454.
(7) Oomens, J.; Polfer, N.; Moore, D. T.; van der Meer, L.; Marshall, A. G.; Eyler, J. R.; Meijer, G.; von Helden, G. *Phys. Chem. Chem. Phys.* **2005**, *7* (7), 1345.
(8) Oh, H.; Breuker, K.; Sze, S.; Ge, Y.; Carpenter, B.; McLafferty, F. *Proc. Natl. Acad. Sci. U. S. A.* **2002**, *99* (25), 15863−15868.
(9) Förster, T. *Ann. Phys.* **1948**, *437* (1−2), 55−75.
(10) Lakowicz, J. R. *Principles of fluorescence spectroscopy*; Springer: New York, 2006.

DOI: 10.1021/acs.analchem.5b01591
Anal. Chem. 2015, 87, 7559−7565

(11) Royer, C. A. *Chem. Rev.* **2006**, *106* (5), 1769−1784.
(12) Schuler, B.; Lipman, E. A.; Eaton, W. A. *Nature* **2002**, *419* (6908), 743−747.
(13) Schuler, B.; Hofmann, H. *Curr. Opin. Struct. Biol.* **2013**, *23* (1), 36−47.
(14) Dehmelt, L.; Bastiaens, P. I. H. *Nat. Rev. Mol. Cell Biol.* **2010**, *11* (6), 440−452.
(15) Danell, A.; Parks, J. H. *Int. J. Mass Spectrom.* **2003**, *229* (1−2), 35−45.
(16) Dashtiev, M.; Azov, V.; Frankevich, V.; Scharfenberg, L.; Zenobi, R. *J. Am. Soc. Mass Spectrom.* **2005**, *16* (9), 1481−1487.
(17) March, R. E.; Todd, J. F. J. *Quadrupole Ion Trap Mass Spectrometry*; J. Wiley: Hoboken, N.J., 2005.
(18) Daly, S.; Poussigue, F.; Simon, A.-L.; MacAleese, L.; Bertorelle, F.; Chirot, F.; Antoine, R.; Dugourd, P. *Anal. Chem.* **2014**, *86* (17), 8798−8804.
(19) Talbot, F. O.; Rullo, A.; Yao, H.; Jockusch, R. A. *J. Am. Chem. Soc.* **2010**, *132* (45), 16156−16164.
(20) Gallagher, T.; Alexander, P.; Bryan, P.; Gilliland, G. *Biochemistry* **1994**, *33* (15), 4721−4729.
(21) Gronenborn, A.; Filpula, D.; Essig, N.; Achari, A.; Whitlow, M.; Wingfield, P.; Clore, G. *Science* **1991**, *253* (5020), 657−661.
(22) Minor, D.; Kim, P. *Nature* **1994**, *371* (6494), 264−267.
(23) Minor, D. L.; Kim, P. S. *Nature* **1996**, *380* (6576), 730−734.
(24) Kobayashi, N.; Honda, S.; Yoshii, H.; Munekata, E. *Biochemistry* **2000**, *39* (21), 6564−6571.
(25) Alexander, P.; Orban, J.; Bryan, P. *Biochemistry* **1992**, *31* (32), 7243−7248.
(26) Park, S. H.; O'Neil, K. T.; Roder, H. *Biochemistry* **1997**, *36* (47), 14277−14283.
(27) McCallister, E. L.; Alm, E.; Baker, D. *Nat. Struct. Biol.* **2000**, *7* (8), 669−673.
(28) Alexander, P.; Fahnestock, S.; Lee, T.; Orban, J.; Bryan, P. *Biochemistry* **1992**, *31* (14), 3597−3603.
(29) Nauli, S.; Kuhlman, B.; Baker, D. *Nat. Struct. Biol.* **2001**, *8* (7), 602−605.
(30) Tokuriki, N.; Stricher, F.; Schymkowitz, J.; Serrano, L.; Tawfik, D. S. *J. Mol. Biol.* **2007**, *369* (5), 1318−1332.
(31) Bian, Q.; Forbes, M. W.; Talbot, F. O.; Jockusch, R. A. *Phys. Chem. Chem. Phys.* **2010**, *12* (11), 2590−2598.
(32) Forbes, M. W.; Talbot, F. O.; Jockusch, R. A. In *Practical Aspects of Trapped Ion Mass Spectrometry: Applications of Ion Trapping Devices*; March, R. E., Todd, J. F. J., Eds.; CRC Press: Boca Raton, Florida, 2009; Vol. *5*, Chapter 9, pp 239−290.
(33) Nagy, A. M.; Talbot, F. O.; Czar, M. F.; Jockusch, R. A. *J. Photochem. Photobiol., A* **2012**, *244*, 47−53.
(34) Talbot, F. O.; Sciuto, S. V.; Jockusch, R. A. *J. Am. Soc. Mass Spectrom.* **2013**, *24* (12), 1823−1832.
(35) Hofmann, H.; Hillger, F.; Pfeil, S. H.; Hoffmann, A.; Streich, D.; Haenni, D.; Nettels, D.; Lipman, E. A.; Schuler, B. *Proc. Natl. Acad. Sci. U. S. A.* **2010**, *107* (26), 11793−11798.
(36) Chowdhury, S.; Katta, V.; Chait, B. *J. Am. Chem. Soc.* **1990**, *112* (24), 9012−9013.
(37) Valentine, S. J.; Counterman, A. E.; Clemmer, D. E. *J. Am. Soc. Mass Spectrom.* **1997**, *8* (9), 954−961.
(38) Dietrich, A.; Buschmann, V.; Muller, C.; Sauer, M. *Rev. Mol. Biotechnol.* **2002**, *82* (3), 211−231.
(39) Antoine, R.; Dugourd, P. *Phys. Chem. Chem. Phys.* **2011**, *13* (37), 16494−16509.
(40) Vonderach, M.; Winghart, M.-O.; MacAleese, L.; Chirot, F.; Antoine, R.; Dugourd, P.; Weis, P.; Hampe, O.; Kappes, M. M. *Phys. Chem. Chem. Phys.* **2014**, *16* (7), 3007−3013.
(41) Hoffmann, A.; Kane, A.; Nettels, D.; Hertzog, D. E.; Baumgaertel, P.; Lengefeld, J.; Reichardt, G.; Horsley, D. A.; Seckler, R.; Bakajin, O.; Schuler, B. *Proc. Natl. Acad. Sci. U. S. A.* **2007**, *104* (1), 105−110.
(42) Breuker, K.; Oh, H. B.; Horn, D. M.; Cerda, B. A.; McLafferty, F. W. *J. Am. Chem. Soc.* **2002**, *124* (22), 6407−6420.
(43) Lillo, M. P.; Szpikowska, B. K.; Mas, M. T.; Sutin, J. D.; Beechem, J. M. *Biochemistry* **1997**, *36* (37), 11273−11281.
(44) Sinha, K. K.; Udgaonkar, J. B. *J. Mol. Biol.* **2007**, *370* (2), 385−405.
(45) Hohng, S.; Joo, C.; Ha, T. *Biophys. J.* **2004**, *87* (2), 1328−1337.

DOI: 10.1021/acs.analchem.5b01591
Anal. Chem. 2015, 87, 7559−7565